Nano Energy 30 (2016) 771–779

Contents lists available at ScienceDirect

Nano Energy

journal homepage: www.elsevier.com/locate/nanoen

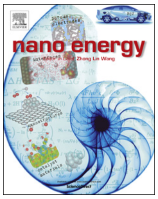

In situ TEM probing of crystallization form-dependent sodiation behavior in ZnO nanowires for sodium-ion batteries

Feng Xu [a,b,*], Zhengrui Li [a], Lijun Wu [b], Qingping Meng [b], Huolin L. Xin [c], Jun Sun [a], Binghui Ge [d], Litao Sun [a,*], Yimei Zhu [b,**]

[a] *SEU-FEI Nano-Pico Center, Key Laboratory of MEMS of the Ministry of Education, Southeast University, Nanjing 210096, China*
[b] *Condensed Matter Physics & Materials Science Department, Brookhaven National Laboratory, Upton, NY 11973, USA*
[c] *Center for Functional Nanomaterials, Brookhaven National Laboratory, Upton, NY 11973, USA*
[d] *Institute of Physics, Chinese Academy of Sciences, Beijing 100190, China*

ARTICLE INFO

Article history:
Received 12 August 2016
Received in revised form
10 September 2016
Accepted 11 September 2016
Available online 13 September 2016

Keywords:
Sodium-ion batteries
In situ transmission electron microscopy
ZnO nanowires
Electrochemical sodiation
Microstructure control

ABSTRACT

Development of sodium-ion battery (SIB) electrode materials currently lags behind electrodes in commercial lithium-ion batteries (LIBs). However, in the long term, development of SIB components is a valuable goal. Their similar, but not identical, chemistries require careful identification of the underlying sodiation mechanism in SIBs. Here, we utilize *in situ* transmission electron microscopy to explore quite different sodiation behaviors even in similar electrode materials through real-time visualization of microstructure and phase evolution. Upon electrochemical sodiation, single-crystalline ZnO nanowires (sc-ZNWs) are found to undergo a step-by-step electrochemical displacement reaction, forming crystalline $NaZn_{13}$ nanograins dispersed in a Na_2O matrix. This process is characterized by a slowly propagating reaction front and the formation of heterogeneous interfaces inside the ZNWs due to non-uniform sodiation amorphization. In contrast, poly-crystalline ZNWs (pc-ZNWs) exhibited an ultrafast sodiation process, which can partly be ascribed to the availability of unobstructed ionic transport pathways among ZnO nanograins. Thus the reaction front and heterogeneous interfaces disappear. The *in situ* TEM results, supported by calculation of the ion diffusion coefficient, provide breakthrough insights into the dependence of ion diffusion kinetics on crystallization form. This points toward a goal of optimizing the microstructure of electrode materials in order to develop high performance SIBs.

1. Introduction

Rechargeable lithium-ion batteries (LIBs) have become a mainstay of the digital age with dominance in portable electronics market. However, for emerging large-scale stationary applications, *e.g.*, electric vehicles, power grid storage, and load leveling, the issue of the limited natural abundance of lithium resource will arise in the immediate future, along with an inevitable cost increase [1]. Therefore, there arises a tremendous interest in alternative metal-ion batteries based on abundant resources. Sodium-ion battery (SIB) has recently attracted significant attention due to the "rocking chair" operating principle similar to the LIB. Moreover, virtually inexhaustible and ubiquitous sodium resources circumvent the geopolitical issue that plague lithium resource [2–5]. Because the chemistries of LIBs and SIBs are similar, the mechanistic insights obtained from the studies of LIBs may be applicable to the SIBs. In this regard, both SIBs and LIBs have shared some of the same cathode materials including layered AMO_2 (M=Co, Ni, Ti), olivine or maricite $AMPO_4$ (M=Fe, Mn, Co, Ni), and the NASICON family of compounds [6,7].

In contrast to the great progress on SIB cathode materials, adapting LIB anode materials to SIBs has been thus far problematic. For example, a graphite anode with an interlayer distance of 1.86 Å may not accommodate the reversible intercalation of Na^+ ions (diameter of 2.04 Å) [8]. As a result, pure graphite forms only a NaC_{64} phase during sodiation, thus resulting in a lower capacity, $\sim 35 mA\,h\,g^{-1}$, compared with $\sim 370\,mA\,h\,g^{-1}$ in the Li-intercalated graphite compound of LiC_6 (stage I). Graphene and hard carbon can circumvent the issue of size [9,10], but their modest specific capacities are insufficient for practical SIB applications. Moreover, the well-studied metal oxide materials in LIBs with high theoretical capacities have also been investigated as viable anode

---

[*] Corresponding authors at: SEU-FEI Nano-Pico Center, Key Laboratory of MEMS of the Ministry of Education, Southeast University, Nanjing 210096, China.

[**] Corresponding author.

E-mail addresses: fxu@seu.edu.cn (F. Xu), slt@seu.edu.cn (L. Sun), zhu@bnl.gov (Y. Zhu).

http://dx.doi.org/10.1016/j.nanoen.2016.09.020
2211-2855/© 2016 Elsevier Ltd. All rights reserved.

materials for SIBs [11–14]. Due to similar, but not identical, chemistries in LIBs and SIBs, however, not all of them possess reliable electrochemical cycleability upon sodiation/desodiation. In this regard, *in situ* transmission electron microscopy (TEM) has been used to probe the failure mechanism of single-crystalline SnO_2 nanowires for SIBs [15], despite its success in LIBs [16,17]. These reactions are difficult or impossible to be understood by ex situ measurements. Thus far, the effort directed toward *in situ* TEM research of SIBs is substantially less than that for LIBs, encouraging us to augment our knowledge of the various electrochemical reaction mechanisms stemming from the inherent characteristics of sodium.

In this paper, we employed state-of-the-art *in situ* TEM to visualize the microstructural evolution and phase transformation and to track ion diffusion during electrochemical sodiation of ZnO nanowires (ZNWs). A slow, step-by-step sodiation process was observed for single-crystalline ZNWs (sc-ZNWs). This process was characterized by a slowly propagating reaction front and the formation of heterogeneous interfaces due to non-uniform sodiation amorphization. In contrast, the sodiation process of poly-crystalline ZNWs (pc-ZNWs), composed of tiny ZnO nanograins, was also investigated, revealing an unexpected, fast sodiation process, thus enabling a better rate performance. Interconnected nanoscale channels among ZnO nanograins in pc-ZNWs are thought to act as unobstructed ionic transport pathways for fast sodium ion diffusion. To the best of our knowledge, this is the first *in situ* work in which otherwise similar electrode materials possibly respond differently during the electrochemical sodiation, depending on their single/poly-crystalline forms. This work provides breakthrough insights into crystallization forms-dependent ion diffusion kinetics and rate performance, which can be used to guide the design of high-performance SIB electrode materials through microstructural control.

2. Experimental section

2.1. *In situ TEM experiment of electrochemical sodiation/desodiation*

The *in situ* electrochemical sodiation experiments were carried out using a Nanofactory TEM-scanning tunneling microscopy (STM) holder in an aberration-corrected JEOL ARM200CF TEM. In a typical experiment, the electrochemical setup consists of individual ZNWs as the working electrode, a layer of Na_2O solid electrolyte, and bulk Na metal as the counter electrode. The ZNWs were glued to the half TEM copper grid with conductive epoxy as the working electrode. A 0.25 mm-thick tungsten (W) wire was cut to produce a fresh tip that was then utilized inside a glove box filled with argon gas to scratch the Na metal surface to fetch fresh Na onto the tip. The layer of Na on the tip of the W wire was served as the counter electrode and sodium source. Both the ZNWs and sodium electrodes were mounted onto a Nanofactory STM-TEM holder inside the glove box. The holder was transferred into the TEM column within several seconds. A native Na_2O layer formed on the surface of Na metal due to the exposure to air. This served as the solid-state electrolyte to allow transport of the Na^+ ions. The Na_2O/Na electrode was mounted on the mobile STM probe, which could be driven to contact the ZNW electrode inside the TEM. Electrochemical sodiation took place when a negative bias was applied to the ZNWs with respect to the sodium metal. This drove Na^+ ions transport through the solid-state Na_2O layer. During the sodiation, electron energy loss spectroscopy (EELS) and electron diffraction (ED) were used to monitor chemical composition and phase transformation. Two advanced Gatan CCDs (Model 894 and Model OneView) were used for imaging and capturing the dynamic sodiation/desodiation process. Additional details are described elsewhere [18–20].

2.2. *Half cell measurement*

Galvanostatic electrochemical performance of the single- and poly-crystalline ZNW anodes was obtained with a 2025-type coin cell in the voltage window of 0.01–2.0 V *versus* Na/Na^+ at room temperature on a Neware battery cycler at various current densities. The working electrode for the SIBs is the slurry mixture of active material (ZnO powder), acetylene black, and polyvinylidene fluoride (PVDF) (75:15:10 weight ratio) in *N*–methyl pyrrolidine (NMP) which had been stirred for 12 h. The slurry was coated onto the Cu current collector and dried at 240 °C for 4 h under Argon gas. The thickness of the electrode without current collector was 20 ± 0.5 μm. Metal sodium foil was used as the counter electrode and reference electrode. The electrolyte consists of 1.0 mol/L $NaPF_4$ in an ethylene carbonate (EC)-diethyl carbonate (DEC) mixture solution (1:1 volume ratio). For the galvanostatic intermittent titration technique (GITT) tests, the coin cells were discharged/charged at C/10 with a current pulse duration of 0.5 h and interval time of 1 h.

3. Results and discussion

The first sodiation process is critical for the battery because this stage could imprint irreversible damage on the electrode materials due to microstructural evolution and phase transformation. To understand the electrochemical behavior of ZnO in SIBs, the sodiation process of individual sc-ZNWs was first observed *in situ*, as shown in Fig. 1 and Movie S1. Fig. 1a presents a schematic illustration of the *in situ* experiment setup that enables direct observation of the electrochemical sodiation of a nano-SIB. The taper-like sc-ZNWs are attached to the copper TEM grid and used as the working electrode. The Na metal attached to the tungsten wire serves as the counter-electrode and sodium source where the naturally oxidized Na_2O and NaOH layer is used as a solid electrolyte. Fig. 1b shows a panoramic TEM image of the constructed nano-SIB inside the TEM. A magnified TEM image of the tip of the pristine ZNW is displayed in the inset of Fig. 1b, showing its taper-like morphology with a taper degree of 1:3. The HRTEM image of the ZnO taper tip in Fig. 1c shows its single-crystal nature with a well-resolved fringe spacing of 0.26 nm, corresponding to the (0002) planes of ZnO. The corresponding fast Fourier transform (FFT) pattern (inset in Fig. 1c) can be indexed as the hexagonal structure of ZnO (JCPDF No. 79-0207).

Supplementary material related to this article can be found online at http://dx.doi.org/10.1016/j.nanoen.2016.09.020.

After contact was established between the two electrodes, the electrochemical sodiation reaction driving the flow of electrons and Na^+ ions across the circuit was initiated by applying a bias of -1.5 V to the sc-ZNW with respect to the Na electrode. The bias voltage was used for all sodiation experiments in this study unless otherwise stated. Fig. 1D-j shows the morphological evolution of the sc-ZNW during the first sodiation. A nanoparticle (marked with a black arrow) on the nanowire is used as object of reference to measure axial elongation of the nanowire. At 0.5 min (Fig. 1d), the sharp tip of the sc-ZNW has completely disappeared due to the sodiation-induced volume expansion. The sodiated region showed a lighter contrast with a length of around 290 nm (the reaction front is marked by a yellow arrow), yielding an average sodiation speed of 580 nm/min along the longitudinal direction of the sc-ZNW. After an additional sodiation of 16 min (Fig. 1i), the displacement of the reaction front was about 1230 nm and the sc-ZNW was elongated by ~30.7%. Unexpectedly, we find that the average sodiation speed varied during the sodiation process. The